Thiol-Induced Etching

International Edition: DOI: 10.1002/anie.201502934
German Edition: DOI: 10.1002/ange.201502934

Radicals Are Required for Thiol Etching of Gold Particles**

*Timothy A. Dreier and Christopher J. Ackerson**

Abstract: *Etching of gold with an excess of thiol ligand is used in both synthesis and analysis of gold particles. Mechanistically, the process of etching gold with excess thiol is unclear. Previous studies have obliquely considered the role of oxygen in thiolate etching of gold. Herein, we show that oxygen or a radical initiator is a necessary component for efficient etching of gold by thiolates. Attenuation of the etching process by radical scavengers in the presence of oxygen, and the restoration of activity by radical initiators under inert atmosphere, strongly implicate the oxygen radical. These data led us to propose an atomistic mechanism in which the oxygen radical initiates the etching process.*

Thiolate-protected gold nanoparticles are of interest for both fundamental and applied research because of their remarkable stability.[1] Synthesis of many "atomically precise" nanoclusters incorporates an etching step in which excess thiolate ligand converts larger particles into smaller and more thermodynamically stable ones.[2] Alternatively, larger nanoparticles may be etched using excess thiol.[3] Syntheses incorporating an etching step, alternatively described as size focusing or digestive ripening, are recently shown to give high yield of many clusters, including $Au_{18}(SR)_{14}$,[4] $Au_{20}(SR)_{16}$,[5] $Au_{23}(SR)_{16}$,[6] $Au_{24}(SR)_{20}$,[5b,7] $Au_{25}(SR)_{18}$,[8] $Au_{28}(SR)_{20}$,[3a,9] $Au_{36}(SR)_{24}$,[10] $Au_{38}(SR)_{24}$,[11] $Au_{40}(SR)_{24}$,[12] $Au_{68}(SR)_{34}$,[13] $Au_{99}(SR)_{42}$,[14] $Au_{144}(SR)_{60}$,[15] $Au_{333}(SR)_{\approx 80}$,[16] and $Au_{\approx 500}(SR)_{\approx 120}$ through tuning of the synthetic conditions.[17] Furthermore, etching is successful in production of alloys of these clusters, including $Au_{24}Pd(SR)_{18}$,[18] $Au_{24}Pt(SR)_{18}$,[19] and $Au_{144-x}Ag_x(SR)_{60}$.[20] Other examples have been reviewed recently.[21] Etching-type mechanisms also presumably underlie many digestive ripening transformations of noble metal nanoparticles.[22] Furthermore, etching is sometimes used to liberate ligands for downstream analysis.

Despite widespread adoption, the mechanism of thiol-induced etching is obscure, even after theoretical and experimental investigation.[11a,23] The literature on magic-number gold nanocluster (AuNC) synthesis suggests an overall reaction as shown in (1), highlighting the importance of etching in arriving at the final products.[24]

$$\begin{aligned} &H^+AuCl_4^-(aq) + (n\text{-Oct})_4N^+Br^-(org) + 3\,RSH \\ &\xrightarrow{\text{Step 1}} (n\text{-Oct})_4N^+AuX_4^-(org) + 3\,RSH(org) + HX(aq) \\ &\xrightarrow{\text{Step 2}} (AuSR)_n + RSSR + (n\text{-Oct})_4N^+ + 4\,X^- + 3\,H^+ \\ &\xrightarrow[\text{Step 3}]{BH_4^-} Au_x(SR)_y \xrightarrow[\text{Step 4}]{\text{etching}} Au_{(x-m)}(SR)_{(y-n)} \end{aligned} \quad (1)$$

Consistent with Reaction (1) are recent reports showing that larger particles are formed as intermediates before the final synthetic product is formed for Au_{25}.[23a] Similarly, etching procedures can convert Au_{40} into Au_{38} or Au_{36}, as well as Au_{102} into Au_{67} and Au_{144} into a variety of smaller clusters.[12b,14,25] Overall, it appears that most synthesis of precisely defined thiolate-protected metal and metal–alloy nanoclusters include a final step in which initially formed polydisperse $Au_x(SR)_y$ nanoparticles are etched to precisely defined $Au_{(x-m)}(SR)_{(y-n)}$ nanoclusters in a mechanistically obscure process.

Gold nanoparticle syntheses are typically performed under ambient atmosphere. We and others observed in a preliminary way that synthesis and etching optimized under ambient atmosphere do not work well when performed under inert atmosphere.[1c,26,27] Intrigued by this observation and the mechanistic obscurity of the process, we endeavored to clarify the role of oxygen in gold nanocluster etching. We chose to examine role of oxygen in the etching of large (colloidal) gold nanoparticles, as well as the role of oxygen in the etching based synthesis of Au_{25}. In each case, we observed oxygen was critical for reaction progress.

The colloidal particles we investigated are 5 nm diameter phosphatidylcholine (PC)-coated Au nanoparticles (PC-AuNPs). These were synthesized by a previously reported procedure, yielding products with a characteristic plasmon resonance at 526 nm.[28] Etching of these colloids proceeded in a calculated 500-fold excess of *n*-hexanethiol to gold atoms in methylene chloride. The progress of etching was determined optically by monitoring the surface plasmon resonance peak. As the particles shrink during etching, the surface plasmon becomes less prominent.[17,29,30]

Figure 1 shows the results of etching of colloidal gold in excess *n*-hexanethiol. The black diamond trace and red square trace depict thiol etching of gold in the presence and absence of O_2, respectively. The O_2 atmosphere was maintained with an O_2 balloon, although similar results are observed if the reaction is performed in a vessel open to atmosphere. This result shows clearly that without O_2, the etching of colloidal particles stalls, whereas in the presence of O_2 the etching can proceed until the nanoparticles are largely converted into gold(I)–thiolate polymeric products.

Since O_2 can serve as a radical initiator, we hypothesized that etching may proceed through a radical based mechanism. To test this, we attempted the etching experiment in toluene (a radical scavenger; Figure 1, blue circle trace). The reactions were sealed and monitored over the course of 90 min.

[*] T. A. Dreier, Dr. C. J. Ackerson
Chemistry, Colorado State University
1847 Campus Deliver, Fort Collins, CO 80523 (USA)
E-mail: Ackerson@colostate.edu

[**] C.J.A. acknowledges support from NIH R21 EB014520. We acknowledge Robert Higgins for assistance with EPR spectroscopy.

Supporting information for this article is available on the WWW under http://dx.doi.org/10.1002/anie.201502934.

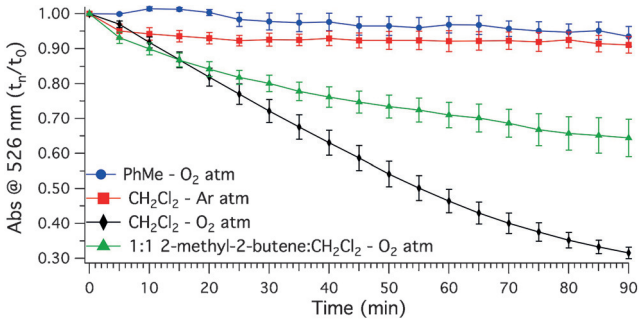

Figure 1. Etching of PC-AuNPs with hexane thiol. Each point is the average of three runs, with error bars showing standard error. Solvents for inert experiments were degassed with three cycles of freeze/pump/thaw. Detailed experimental information and raw data provided in the Supporting Information.

Table 1: Additive and atmosphere effects.

Entry	Atmosphere	Additive	Equiv to Au	Equiv to $NaBH_4$	% Yield[a] $Au_{25}(PET)_{18}$
1	ambient	none	N/A	N/A	60.0
2	ambient	BHT[b]	10.1	1.00	49.3
3	argon[c]	AIBN[d]	1.00	0.250	40.9
4	ambient	BHT	20.2	2.00	10.6
5	ambient	BHT	30.2	3.00	7.00
6	ambient	BHT	40.3	4.00	7.45
7	argon[c]	none	N/A	N/A	0.00

[a] To $HAuCl_4 \cdot 3\,H_2O$. [b] 3,5-di-*tert*-butyl-4-hydroxytoluene. [c] All solutions were degassed by three cycles of freeze/pump/thaw. [d] Azobisisobutyronitrile.

Etching in toluene is minimal and comparable to etching in oxygen-free CH_2Cl_2.

Correspondingly, including a radical scavenger, 2-methyl-2-butene, as a co-solvent with dichloromethane inhibits etching (Figure 1, green triangle trace). Together, these data suggest that etching of colloidal gold nanoparticles by thiolates proceeds through a radical-based mechanism.

To determine if our findings are specific to the colloidal system or generalizable to all thiol etching of gold, we examined the well-developed etching-based Au_{25} synthesis in closer detail.[1c] We first by investigated whether Au-thiolate polymer formation (Reaction (1), step 2) depends on the presence of oxygen. The oligomer/polymer was synthesized by mixing $HAuCl_4 \cdot 3\,H_2O$ in THF with 1.12 equiv of TOAB, followed by addition of phenylethanethiol (PET) in THF through a syringe. We attempted this synthesis under both ambient atmosphere, and with degassed components under argon atmosphere.

Success of Au^I–PET oligomer formation in this case was determined by examination of resulting ^1H and ^{13}C NMR spectra. These spectra were distinct from the starting materials, and identical (Supporting Information, Figures S20 and S21), indicating that oxygen is not involved in the formation of Au^I–PET oligomers/polymers.

We next determined the O_2 dependence of the simultaneous reduction and etching steps of $Au_{25}(SR)_{18}$ synthesis (Reaction (1), step 4). All solvents were degassed by three cycles of freeze/pump/thaw with an argon atmosphere maintained during the course of the reaction. Success of $Au_{25}(SR)_{18}$ formation was determined by production of a product with a linear optical spectrum consistent with previous reports (Supporting Information, Figure S15). When oxygen is excluded from the reduction/etching step, the reaction fails to produce $Au_{25}(SR)_{18}$ (Table 1 Entry 7; Supporting Information, Figure S18), consistent with a previous report.[1c] The resulting spectrum of this reduction/etching step is featureless, indicating particles larger than Au_{25} but too small to be plasmonic (Supporting Information, Figure S19).[30]

To test if the radical nature of oxygen is key to the reduction/etching step, we added a radical initiator to the anaerobic synthesis. The particular radical initator, azobisisobutyronitrile (AIBN, a common initiator in radical polymerizations) was added just prior to the addition of $NaBH_4$ in the previously described anaerobic reaction. Consistent with our hypothesis, this reaction gave $Au_{25}(PET)_{18}$ in 40.9 % yield (Table 1, Entry 3), consistent with yields typical in aerobic synthesis of $Au_{25}(SR)_{18}$.[1b,31]

Conversely, we found that inclusion of a radical scavenger in the aerobic synthesis diminished product yield. We added varying amounts of 3,5-di-*tert*-butyl-4-hydroxytoluene (BHT, a radical inhibitor) to the reaction under ambient conditions, again just prior to addition of $NaBH_4$. We observed that BHT in excess of borohydride substantially reduced the reaction yield of Au_{25} (Table 1, entries 2, 4–6). Notably, 3 and 4 equivalents of BHT to $NaBH_4$ (entries 4 and 6, respectively) gave very nearly the same result. This may be due to saturation of the THF with BHT.

The overall synthesis of thiolate-protected gold nanoparticles, as depicted in Reaction (1), proceeds in four steps. Following formation of an oligomer (steps 1 and 2), AuNPs are formed from the oligomer via reduction by sodium borohydride (step 3). This initial mixture of polydisperse nanoparticles is then etched to the final product (step 4). Theoretical study of thiolate protected nanoparticle synthesis so far focuses on the initial growth.[23d,32] This previous theoretical work suggests that initial growth from the oligomeric species (Reaction (1), step 3) proceeds by a hydride transfer from $NaBH_4$ to Au^I to give the large and polydisperse AuNPs reported by Dass.[23a] The mechanism of etching (Reaction (1), step 4), which is key to arriving at a magic number cluster, is presently obscure.

We propose that the etching of AuNPs into more focused size distributions is the oxygen-dependent portion of the synthesis, and that it is the radical character of oxygen that is important. In Scheme 1, we propose a radical-based mechanism for etching of AuNPs. After formation of large AuNPs from $NaBH_4$ reduction of the Au^I–thiolate oligomer, the disulfide that is formed in the initial step of the synthesis and excess $NaBH_4$ remains in solution. We propose that borohydride reduces the disulfide to the free thiol, from which the O_2 radical abstracts a proton to give a thiyl radical (**1**) and $HOO^{\bullet}$.

The thiyl radical then homolytically cleaves a sulfur–gold bond on the surface of the initial AuNC to expose core Au^0. This newly exposed Au^0 is oxidized by the peroxy radical formed in the first step, to give a new solvent-exposed Au^I

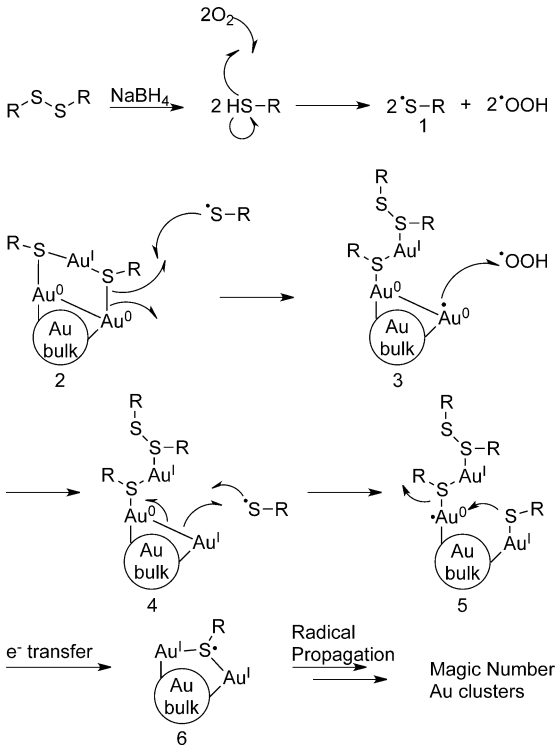

Scheme 1. Proposed etching mechanism.

atom (**3**). Homolytic cleavage of an Au–Au bond gives **5**, in which another equivalent of thiol is now attached to the cluster. Breaking of the Au–S bond in **5** liberates an Au-thiolate monomer and gives another surface-exposed Au^I. Formation of a new Au–S bond gives **6**, in which one layer of Au has been removed from the starting cluster. This cycle can repeat, etching all AuNPs in a preparation to thermodynamically stable magic number AuNCs.

Along with the radical initiation and scavenging experiments, we performed spin-trapping EPR (ESR) spectroscopy using DMPO[33] as the spin trap. The ESR spectrum (Supporting Information, Figure S23) is consistent with an Au radical as depicted in **3**, this offers further evidence for our mechanistic proposal.

Omission of O_2 makes the mechanism in Scheme 1 impossible. Correspondingly, the large insoluble products observed by Murray would be the expected result of inert synthesis where etching cannot proceed.[1c] The addition of AIBN allows for formation of a hydroxyl radical,[34] which can then take the place of the peroxy radical and initiate the etching reaction. AIBN can also initiate formation of the needed thiyl radical, with these two species then intercepting the mechanism proposed in Scheme 1 (Supporting Information, Figure S22).

Overall our data strongly suggest that the necessity for oxygen in both thiol-etching of colloidal gold and in Brust-type syntheses of AuNCs arises from the O_2 diradical. Although molecular oxygen has been shown to react with thiols to give thiyl radicals,[35] to the best of our knowledge this is the first systematic investigation into the role of oxygen and other radicals in AuNC synthesis with thiols. While radicals are known to etch AuNPs under Fenton-like conditions,[36] Scheme 1 represents the first proposed atomistic mechanism for thiolate etching of AuNPs so far as we are aware.

Full understanding of this process may allow for better control of reaction outcomes, that is, size control of particles via changes to the reaction atmosphere. Better control over reproducibility, size, and dispersity in these processes will allow for a deeper investigation into the size-dependent properties of magic-number AuNCs, which in turn will broaden the scope of their applications.

Keywords: etching · gold nanoclusters · nanoparticles · thiolates

How to cite: *Angew. Chem. Int. Ed.* **2015**, *54*, 9249–9252
Angew. Chem. **2015**, *127*, 9381–9384

[1] a) H. Häkkinen, *Chem. Soc. Rev.* **2008**, *37*, 1847–1859; b) J. F. Parker, C. A. Fields-Zinna, R. W. Murray, *Acc. Chem. Res.* **2010**, *43*, 1289–1296; c) J. F. Parker, J. E. F. Weaver, F. McCallum, C. A. Fields-Zinna, R. W. Murray, *Langmuir* **2010**, *26*, 13650–13654; d) Y. Zhu, H. Qian, M. Zhu, R. Jin, *Adv. Mater.* **2010**, *22*, 1915–1920; e) Y. Zhu, R. Jin, Y. Sun, *Catalysts* **2011**, *1*, 3–17; f) M. A. Tofanelli, C. J. Ackerson, *J. Am. Chem. Soc.* **2012**, *134*, 16937–16940.

[2] M. Brust, M. Walker, D. Bethell, D. J. Schiffrin, R. Whyman, *J. Chem. Soc. Chem. Commun.* **1994**, 801–802.

[3] a) T. G. Schaaff, G. Knight, M. N. Shafigullin, R. F. Borkman, R. L. Whetten, *J. Phys. Chem. B* **1998**, *102*, 10643–10646; b) T. G. Schaaff, R. L. Whetten, *J. Phys. Chem. B* **1999**, *103*, 9394–9396.

[4] a) Q. Yao, Y. Yu, X. Yuan, Y. Yu, J. Xie, J. Y. Lee, *Small* **2013**, *9*, 2696–2701; b) A. Das, C. Liu, H. Y. Byun, K. Nobusada, S. Zhao, N. Rosi, R. Jin, *Angew. Chem. Int. Ed.* **2015**, *127*, 3140–3144; *Angew. Chem.* **2015**, *127*, 3183–3187; c) Q. Tang, D.-e. Jiang, *J. Phys. Chem. C* **2015**, *119*, 2904–2909.

[5] a) Y. Pei, Y. Gao, N. Shao, X. C. Zeng, *J. Am. Chem. Soc.* **2009**, *131*, 13619–13621; b) X. Meng, Z. Liu, M. Zhu, R. Jin, *Nanoscale Res. Lett.* **2012**, *7*, 277; c) X. Zhu, S. Jin, S. Wang, X. Meng, C. Zhu, M. Zhu, R. Jin, *Chem. Asian J.* **2013**, *8*, 2739–2745.

[6] a) M. A. H. Muhammed, P. K. Verma, S. K. Pal, R. C. A. Kumar, S. Paul, R. V. Omkumar, T. Pradeep, *Chem. Eur. J.* **2009**, *15*, 10110–10120; b) A. Das, T. Li, K. Nobusada, C. Zeng, N. L. Rosi, R. Jin, *J. Am. Chem. Soc.* **2013**, *135*, 18264–18267; c) M. Hesari, M. S. Workentin, *J. Mater. Chem. C* **2014**, *2*, 3631–3638.

[7] a) M. Zhu, H. Qian, R. Jin, *J. Phys. Chem. Lett.* **2010**, *1*, 1003–1007; b) D. Crasto, G. Barcaro, M. Stener, L. Sementa, A. Fortunelli, A. Dass, *J. Am. Chem. Soc.* **2014**, *136*, 14933–14940; c) A. Das, T. Li, G. Li, K. Nobusada, C. Zeng, N. L. Rosi, R. Jin, *Nanoscale* **2014**, *6*, 6458–6462; d) Q. Tang, R. Ouyang, Z. Tian, D.-e. Jiang, *Nanoscale* **2015**, *7*, 2225–2229.

[8] Z. Wu, J. Suhan, R. Jin, *J. Mater. Chem.* **2009**, *19*, 622–626.

[9] a) S. Knoppe, S. Malola, L. Lehtovaara, T. Bürgi, H. Häkkinen, *J. Phys. Chem. A* **2013**, *117*, 10526–10533; b) C. Zeng, T. Li, A. Das, N. L. Rosi, R. Jin, *J. Am. Chem. Soc.* **2013**, *135*, 10011–10013; c) D. M. Chevrier, C. Zeng, R. Jin, A. Chatt, P. Zhang, *J. Phys. Chem. C* **2015**, *119*, 1217–1223.

[10] a) P. R. Nimmala, A. Dass, *J. Am. Chem. Soc.* **2011**, *133*, 9175–9177; b) C. Zeng, H. Qian, T. Li, G. Li, N. L. Rosi, B. Yoon, R. N. Barnett, R. L. Whetten, U. Landman, R. Jin, *Angew. Chem. Int. Ed.* **2012**, *51*, 13114–13118; *Angew. Chem.* **2012**, *124*, 13291–13295; c) P. R. Nimmala, S. Knoppe, V. R. Jupally, J. H. Delcamp, C. M. Aikens, A. Dass, *J. Phys. Chem. B* **2014**, *118*, 14157–14167; d) A. Das, C. Liu, C. Zeng, G. Li, T. Li, N. L. Rosi, R. Jin, *J. Phys. Chem. A* **2014**, *118*, 8264–8269.

[11] a) H. Qian, Y. Zhu, R. Jin, *ACS Nano* **2009**, *3*, 3795 – 3803; b) H. Qian, M. Zhu, U. N. Andersen, R. Jin, *J. Phys. Chem. A* **2009**, *113*, 4281 – 4284; c) H. Qian, W. T. Eckenhoff, Y. Zhu, T. Pintauer, R. Jin, *J. Am. Chem. Soc.* **2010**, *132*, 8280 – 8281; d) S. Theivendran, A. D. Antony Sami, American Chemical Society, Washington, **2014**, pp. SERMACS-686; e) H. Qian, *Pure Appl. Chem.* **2014**, *86*, 27 – 37.
[12] a) D.-e. Jiang, M. Walter, *Phys. Rev. B* **2011**, *84*, 193402; b) P. R. Nimmala, V. R. Jupally, A. Dass, *Langmuir* **2014**, *30*, 2490 – 2497.
[13] A. Dass, *J. Am. Chem. Soc.* **2009**, *131*, 11666 – 11667.
[14] P. R. Nimmala, A. Dass, *J. Am. Chem. Soc.* **2014**, *136*, 17016 – 17023.
[15] H. Qian, R. Jin, *Chem. Mater.* **2011**, *23*, 2209 – 2217.
[16] H. Qian, Y. Zhu, R. Jin, *Proc. Natl. Acad. Sci. USA* **2012**, *109*, 696 – 700, S696/691 – S696/693.
[17] C. Kumara, X. Zuo, J. Ilavsky, K. W. Chapman, D. A. Cullen, A. Dass, *J. Am. Chem. Soc.* **2014**, *136*, 7410 – 7417.
[18] a) Y. Negishi, W. Kurashige, Y. Niihori, T. Iwasa, K. Nobusada, *Phys. Chem. Chem. Phys.* **2010**, *12*, 6219 – 6225; b) A. Yang, F. Wei, J. Dong, *J. Phys. Chem. A* **2010**, *114*, 4031 – 4035.
[19] H. Qian, D.-e. Jiang, G. Li, C. Gayathri, A. Das, R. R. Gil, R. Jin, *J. Am. Chem. Soc.* **2012**, *134*, 16159 – 16162.
[20] a) S. Malola, H. Hakkinen, *J. Phys. Chem. Lett.* **2011**, *2*, 2316 – 2321; b) C. Kumara, A. Dass, *Nanoscale* **2011**, *3*, 3064 – 3067.
[21] R. Jin, *Nanoscale* **2015**, *7*, 1549 – 1565.
[22] B. L. V. Prasad, S. I. Stoeva, C. M. Sorensen, K. J. Klabunde, *Chem. Mater.* **2003**, *15*, 935 – 942.
[23] a) A. C. Dharmaratne, T. Krick, A. Dass, *J. Am. Chem. Soc.* **2009**, *131*, 13604 – 13605; b) R. Jin, H. Qian, Z. Wu, Y. Zhu, M. Zhu, A. Mohanty, N. Garg, *J. Phys. Chem. Lett.* **2010**, *1*, 2903 – 2910; c) E. B. Guidez, A. Hadley, C. M. Aikens, *J. Phys. Chem. C* **2011**, *115*, 6305 – 6316; d) B. M. Barngrover, C. M. Aikens, *J. Am. Chem. Soc.* **2012**, *134*, 12590 – 12595.
[24] S. R. K. Perala, S. Kumar, *Langmuir* **2013**, *29*, 9863 – 9873.
[25] a) V. R. Jupally, A. Dass, *Phys. Chem. Chem. Phys.* **2014**, *16*, 10473 – 10479; b) P. R. Nimmala, B. Yoon, R. L. Whetten, U. Landman, A. Dass, *J. Phys. Chem. A* **2013**, *117*, 504 – 517.
[26] O. A. Wong, W. S. Compel, C. J. Ackerson, *ACS Comb. Sci.* **2014**, *17*, 11 – 18.
[27] Personal communication with Roger D. Kornberg.
[28] S. Sitaula, M. R. Mackiewicz, S. M. Reed, *Chem. Commun.* **2008**, 3013 – 3015.
[29] R. Philip, P. Chantharasupawong, H. Qian, R. Jin, J. Thomas, *Nano Lett.* **2012**, *12*, 4661 – 4667.
[30] S. Malola, L. Lehtovaara, J. Enkovaara, H. Häkkinen, *ACS Nano* **2013**, *7*, 10263 – 10270.
[31] a) X. Yuan, B. Zhang, Z. Luo, Q. Yao, D. T. Leong, N. Yan, J. Xie, *Angew. Chem. Int. Ed.* **2014**, *53*, 4623 – 4627; *Angew. Chem.* **2014**, *126*, 4711 – 4715; b) X. Yuan, Y. Yu, Q. Yao, Q. Zhang, J. Xie, *J. Phys. Chem. Lett.* **2012**, *3*, 2310 – 2314.
[32] B. M. Barngrover, C. M. Aikens, *J. Phys. Chem. Lett.* **2011**, *2*, 990 – 994.
[33] 5,5-dimethyl-pyrroline-*N*-oxide.
[34] The final solvent mixture for the Brust synthesis ends up to be about 7:2 THF:water, meaning there is sufficient water in the reaction for this to occur.
[35] a) A. L. J. Beckwith, B. S. Low, *J. Chem. Soc.* **1961**, 1304 – 1311; b) E. Banchereau, S. Lacombe, J. Ollivier, *Tetrahedron Lett.* **1995**, *36*, 8197 – 8200; c) X. Baucherel, J. Uziel, S. Juge, *J. Org. Chem.* **2001**, *66*, 4504 – 4510; d) K. J. Tan, U. Wille, *Chem. Commun.* **2008**, 6239 – 6241; e) T. Nauser, W. H. Koppenol, C. Schoneich, *J. Phys. Chem. B* **2012**, *116*, 5329 – 5341.
[36] Z. Zhang, Z. Chen, D. Pan, L. Chen, *Langmuir* **2015**, *31*, 643 – 650.

Received: March 30, 2015
Revised: May 27, 2015
Published online: June 18, 2015

